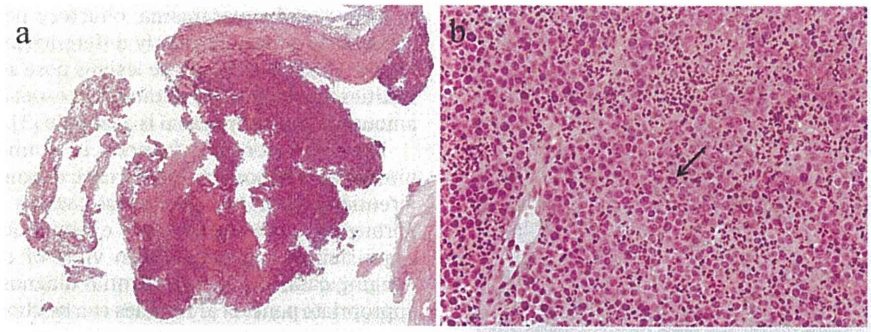

Fig. 3. Representative histologic images. (a) Sheets of undifferentiated malignant cells with focal necrosis are visible. (b) The tumor cells had round to oval nuclei with vesicular chromatin, prominent nucleoli, and scant cytoplasm. Frequent mitotic figures are visible (arrow).

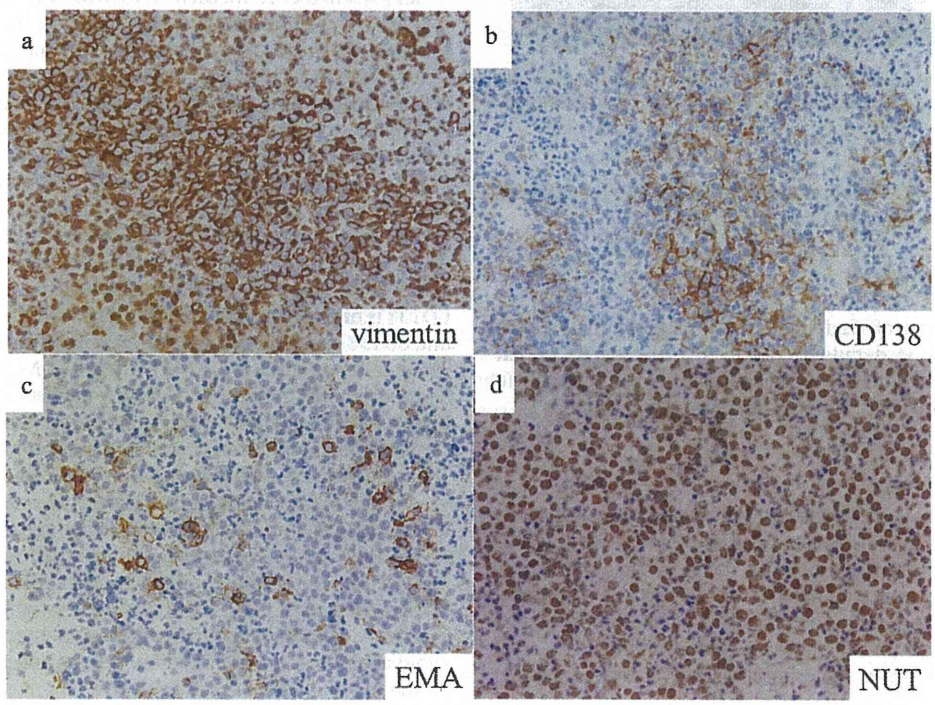

Fig. 4. Immunohistochemical findings of the NUT midline carcinoma. (a) Tumor cells show strong vimentin immunoreactivity. (b) The tumor cells are focally positive for CD138. (c) Positive staining for EMA was observed in a few tumor cells. (d) Immunohistochemistry shows a nuclear staining pattern for NUT.

results were obtained for S-100, CD34, CD99, neuron-specific enolase, CD56, synaptophysin, myogenin, desmin, PLAP, c-kit, hCG, and CD45. A diagnosis of "malignant tumor with necrosis" was made. Because of the strong vimentin positivity and focal positivity for CD138, additional immunohistochemical analyses, in situ hybridization (ISH), and a chromosome analysis were performed to enable a differential diagnosis of poorly differentiated carcinoma and plasmacytoma. ISH showed no staining for Epstein–Barr virus (EBV)-encoded RNA or the kappa and lambda light chains of immunoglobulins. These findings suggested a diagnosis of poorly differentiated carcinoma, rather than plasmacytoma. In addition, immunohistochemistry showed a nuclear staining pattern for NUT (Fig. 4d) and focal positivity for p63. A chromosome analysis identified a 46, XX, t(15;19)(q14;p13) pattern in all 9 cells (Fig. 5). These results strongly suggested a NUT midline carcinoma.

Next, FISH and RT-PCR were performed to confirm the rearrangement of *BRD4* and *NUT*. A FISH analysis revealed the break apart of *NUT* and the fusion of *BRD4* and *NUT* (Fig. 6). Direct sequencing of the 1152-bp fragments (Fig. 7a) showed that nt 2380 of *BRD4* (accession number AF386649) was fused with nt 172 of *NUT*

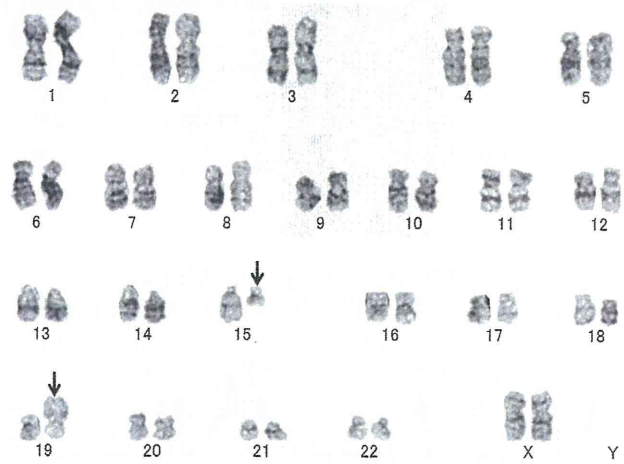

Fig. 5. Karyotype demonstrating the t(15;19)(q14;p13). The derivative chromosomes formed from the translocation are indicated by the arrows.

Fig. 6. Representative finding of FISH. A dual-color FISH analysis shows the fusion gene as a single yellow (overlapping) signal (arrow), including an orange (*BRD4*) and green (*NUT*) signal.

(accession number AF482429) in frame (Fig. 7b). These results confirmed the rearrangement of *BRD4* and *NUT*.

Treatment and follow up

The patient was transferred to another hospital to undergo chemoradiotherapy (the details of which are unknown), which resulted in the almost complete disappearance of the tumor. The patient is alive and well at 12 months after her diagnosis.

Discussion

The histologic features of NMC are, unfortunately, not pathognomonic, since the morphology is that of a poorly differentiated carcinoma with or without squamous differentiation [2–4,10,19]. Several malignant tumors occurring in the sinonasal tract may exhibit an undifferentiated morphology [3,6,20]. The differential diagnosis of these tumors includes hemato-lymphoid malignancies, melanomas, Ewing sarcoma/primitive neuroectodermal

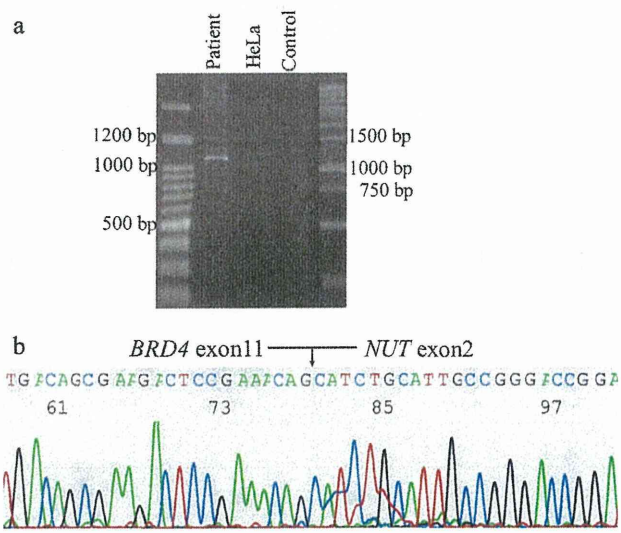

Fig. 7. Detection of BRD4-NUT. (a) PCR amplification (1152 bp) with BR2276F and *NUT*1194R primers. (b) Partial sequence chromogram showing the in-frame fusion of BRD4 exon11 with NUT exon2.

tumors, rhabdomyosarcoma, olfactory neuroblastoma, and germ cell tumors as well as poorly differentiated carcinomas, including NMC [3,6,20]. Overall, these lesions pose significant diagnostic difficulties for the surgical pathologist, especially when only a limited amount of biopsy material is available [3].

Based on recent advances in immunohistochemistry and molecular diagnostics, the current diagnostic strategy for undifferentiated tumors of the nasal cavities has been proposed [6]. Through careful microscopic examination of hematoxylin and eosin-stained sections, and in view of clinical information and imaging data, a list of differential diagnoses can be made and an appropriate panel of antibodies can be chosen to further categorize the tumor. An initial panel including cytokeratins, synaptophysin, S-100 protein, desmin, and CD45 may allow the classification of most lesions or may help to narrow the list of differential diagnoses [6]. Further refinement can be obtained through second-line markers, including ISH for EBV, other neuroendocrine markers, melanocytic markers, myogenin, CD99, other lymphocyte markers, CD138, and light chains [6]. Finally, immunohistochemistry with NUT antibodies [11] can differentiate NMC from other tumors, and molecular analysis can further assist in the recognition of a *NUT* rearrangement, which is specific for NMC [3,7–9,12,19,23].

As described above, the immunohistochemical findings in our case, including strong vimentin positivity and focal positivity for CD138, only spotty positivity for cytokeratin AE1/AE3 and EMA, and negativity for other markers, shortened the list of differential diagnoses to two: poorly differentiated carcinoma and plasmacytoma. CD138 is highly expressed by epithelial cells, as well as plasma cells, and CD138 expression is associated with the differentiation of squamous cell carcinoma [15,17,18]. The *BRD4-NUT* fusion gene encodes a protein that is thought to be involved in the blockage of epithelial differentiation and squamous maturation [9]. In addition, our case showed a poor differentiation, without squamous differentiation. Together, these results led us to expect that the expression of CD138 would be almost absent in our case. However, our case was positive for CD138, but only spotty for other epithelial markers such as AE1/AE3 and EMA. These results made a differential diagnosis more difficult, although the results encouraged us to perform immunohistochemistry using NUT antibodies, which eventually led to a diagnosis of NMC. The accumulation of more cases is needed to avoid achieving a correct diagnosis in a roundabout manner based on the histological features of NMCs.

The *NUT* promoter is active only in adult testis and ciliary ganglion [7,10,20]. As a result, only one of the two fusion genes, e.g., *BRD-NUT* (where the BRD4 promoter and the bromodomains drive the aberrant NUT expression and chromatin binding), but not *NUT-BRD*, is expressed [10]. Until recently, a definitive diagnosis of NMC was made by demonstrating a *NUT* rearrangement using dual color, split-apart FISH using probes flanking *NUT* or by demonstrating a *BRD4-NUT* fusion transcript using RT-PCR [11]. In approximately two-thirds of cases, *NUT* is fused to *BRD4*, forming the *BRD4-NUT* fusion gene [7,10]. The remaining one-third of cases are *NUT*-variants, where the partner gene is *BRD3* or some other uncharacterized gene [8,9]. Whether *NUT*-variant carcinomas differ in outcome, compared with *BRD4-NUT* carcinomas, remains controversial [1,8,10]. To demonstrate the fusion genes, FISH is preferred from a practical perspective because it is capable of detecting all NMCs, including all *NUT*-variants, whereas RT-PCR can currently only detect *BRD3*- or *BRD4-NUT* tumors [10]. Thus, information concerning the breakpoints in the *BRD* or *NUT* genes using RT-PCR direct sequencing is scarce: only four reports have successfully defined the breakpoints of the genes in clinical specimens using direct sequencing [7,9,12,23]. The breakpoints occurred within exon10 of *BRD4* [7], exon11 of *BRD4* [12,23], exon10b of *BRD4* [9], or exon9 of *BRD3* [9], and exon2 of *NUT*, fusing the business end of *BRD4*, encoding both acetyl-histone binding bromodomains and

the extraterminal domain, with virtually the entire *NUT* gene. Our case showed that exon11 of *BRD4* was fused in-frame to exon2 of *NUT*, similar to a Japanese case with pulmonary NMC [23]. It is possible that improved identification of the breakpoints of the targeted gene might reveal an association between variations in the breakpoints and the clinicopathological features, including the location of tumors, the race of patients, the responsiveness to therapies, and the degree of squamous differentiation.

The specific NUT monoclonal antibody has been very recently established [11]. The immunohistochemical staining had a sensitivity of 87%, a specificity of 100%, a negative predictive value of 99%, and a positive predictive value of 100% [11]. The commercial circulation of this highly sensitive and specific NUT monoclonal antibody [11] has facilitated the unambiguous diagnosis of NMC, making it possible to assess the frequency and prognosis of NMC amongst a large population of patients [1,2]. One previous report showed that 3 (2%) of 151 primary sinonasal carcinomas were NMCs [2]. In this previous report, most of the patients who were younger than 50 years old and were diagnosed as having sinonasal undifferentiated carcinoma (3 out of 4, 75%) were found to actually have NMCs. Thus, the inclusion of NUT immunostaining as a part of the diagnostic workup for any sinonasal carcinoma with an undifferentiated component is recommended. Another study, the largest cohort of patients with NMC, showed that the median overall survival for patients was 6.7 months [1]. The 2-year progression-free survival (PFS) was 9%, and the 2-year overall survival (OS) was 19%. A multivariate analysis suggested that the extent of surgical resection and the initial radiotherapy were independent predictors of the PFS and OS, whereas no chemotherapeutic regimen improved the outcome [1]. Our patient underwent chemoradiotherapy (the details of which are unknown), which resulted in the almost complete disappearance of the tumor. Careful follow up is needed to evaluate the effectiveness of this treatment.

Data from the growing number of identified cases can be used to develop effective targeted therapies. One candidate therapy is a bromodomain inhibitor. A study [9] using NMC cell lines showed that the knockdown of the NUT fusions resulted in the dramatic differentiation and growth arrest of the malignant cells. Furthermore, the bromodomain inhibitor JQ1 was shown to be capable of displacing the *BRD4-NUT* fusion protein from chromatin, inducing a rapid differentiation and arrest of proliferation in NUT midline carcinoma cell lines [5]. In addition, JQ1 showed an excellent efficacy in murine xenograft models of NUT midline carcinoma, resulting in tumor differentiation and regression and an increase in survival [5]. The clinical translation of this research requires robust, histological outcome data, including information regarding the association between the breakpoints of the targeted genes and the sensitivity to new drugs.

In this article, we have described a new Japanese case with NMC in the nasal cavity that is pertinent to the expansion of knowledge regarding this rare tumor. Furthermore, the identification of the *BRD4-NUT* fusion gene using direct sequencing in this tumor has provided new insight as to its influence on clinicopathological features, including the location of tumors, the race of patients, the degree of squamous differentiation, and the responsiveness to therapy.

Conflict of interest

The authors have no conflicts of interest to declare.

Acknowledgments

We appreciate the technical assistance of Ms. Kiyoko Nagura and Mr. Hisaki Igarashi.

This case was presented at the Japanese Pathological Society Chubu Meeting on July 13–14, 2013, in Nagoya.

This contribution was supported, in part, by Grants-in-Aid for the U.S.-Japan Cooperative Medical Science Program; the National Cancer Center Research and Development Fund; Grant for priority areas from the Japanese Ministry of Education, Culture, Sports, Science and Technology [221S0001]; and Grants-in-Aid for Cancer Research from the Japanese Ministry of Health, Labor and Welfare [23120201 and 10103838], the Smoking Research Foundation, and the Princess Takamatsu Cancer Research Fund.

References

[1] D.E. Bauer, C.M. Mitchell, K.M. Strait, C.S. Lathan, E.B. Stelow, S.C. Luer, S. Muhammed, A.G. Evans, L.M. Sholl, J. Rosai, E. Giraldi, R.P. Oakley, C. Rodriguez-Galindo, W.B. London, S.E. Sallan, J.E. Bradner, C.A. French, Clinicopathologic features and long-term outcomes of NUT midline carcinoma, Clin. Cancer Res. 18 (2012) 5773–5779.

[2] J.A. Bishop, W.H. Westra, NUT midline carcinomas of the sinonasal tract, Am. J. Surg. Pathol. 36 (2012) 1216–1221.

[3] B.N. Davis, R.G. Karabakhtsian, A.L. Pettigrew, S.M. Arnold, C.A. French, Y.M. Brill, Nuclear protein in testis midline carcinomas: a lethal and underrecognized entity, Arch. Pathol. Lab. Med. 135 (2011) 1494–1498.

[4] A.G. Evans, C.A. French, M.J. Cameron, C.D. Fletcher, D.M. Jackman, C.S. Lathan, L.M. Sholl, Pathologic characteristics of NUT midline carcinoma arising in the mediastinum, Am. J. Surg. Pathol. 36 (2012) 1222–1227.

[5] P. Filippakopoulos, J. Qi, S. Picaud, Y. Shen, W.B. Smith, O. Fedorov, E.M. Morse, T. Keates, T.T. Hickman, I. Felletar, M. Philpott, S. Munro, M.R. McKeown, Y. Wang, A.L. Christie, N. West, M.J. Cameron, B. Schwartz, T.D. Heightman, N. La Thangue, C.A. French, O. Wiest, A.L. Kung, S. Knapp, J.E. Bradner, Selective inhibition of BET bromodomains, Nature 468 (2010) 1067–1073.

[6] A. Franchi, A. Palomba, A. Cardesa, Current diagnostic strategies for undifferentiated tumours of the nasal cavities and paranasal sinuses, Histopathology 59 (2011) 1034–1045.

[7] C.A. French, I. Miyoshi, I. Kubonishi, H.E. Grier, A.R. Perez-Atayde, J.A. Fletcher, BRD4-NUT fusion oncogene: a novel mechanism in aggressive carcinoma, Cancer Res. 63 (2003) 304–307.

[8] C.A. French, J.L. Kutok, W.C. Faquin, J.A. Toretsky, C.R. Antonescu, C.A. Griffin, V. Nose, S.O. Vargas, M. Moschovi, F. Tzortzatou-Stathopoulou, I. Miyoshi, A.R. Perez-Atayde, J.C. Aster, J.A. Fletcher, Midline carcinoma of children and young adults with NUT rearrangement, J. Clin. Oncol. 22 (2004) 4135–4139.

[9] C.A. French, C.L. Ramirez, J. Kolmakova, T.T. Hickman, M.J. Cameron, M.E. Thyne, J.L. Kutok, J.A. Toretsky, A.K. Tadavarthy, U.R. Kees, J.A. Fletcher, J.C. Aster, BRD-NUT oncoproteins: a family of closely related nuclear proteins that block epithelial differentiation and maintain the growth of carcinoma cells, Oncogene 27 (2008) 2237–2242.

[10] C.A. French, NUT midline carcinoma, Cancer Genet. Cytogenet. 203 (2010) 16–20.

[11] H. Haack, L.A. Johnson, C.J. Fry, K. Crosby, R.D. Polakiewicz, E.B. Stelow, S.M. Hong, B.E. Schwartz, M.J. Cameron, M.A. Rubin, M.C. Chang, J.C. Aster, C.A. French, Diagnosis of NUT midline carcinoma using a NUT-specific monoclonal antibody, Am. J. Surg. Pathol. 33 (2009) 984–991.

[12] N. Haruki, K.S. Kawaguchi, S. Eichenberger, P.P. Massion, A. Gonzalez, A.F. Gazdar, J.D. Minna, D.P. Carbone, T.P. Dang, Cloned fusion product from a rare t(15;19)(q13.2;p13.1) inhibit S phase in vitro, J. Med. Genet. 42 (2005) 558–564.

[13] M.S. Hsieh, C.A. French, C.W. Liang, C.H. Hsiao, NUT midline carcinoma: case report and review of the literature, Int. J. Surg. Pathol. 19 (2011) 808–812.

[14] I. Kubonishi, N. Takehara, J. Iwata, H. Sonobe, Y. Ohtsuki, T. Abe, I. Miyoshi, Novel t(15;19)(q15;p13) chromosome abnormality in a thymic carcinoma, Cancer Res. 51 (1991) 3327–3328.

[15] H. Kurokawa, M. Zhang, S. Matsumoto, Y. Yamashita, T. Tanaka, K. Takamori, K. Igawa, M. Yoshida, H. Fukuyama, T. Takahashi, S. Sakoda, Reduced syndecan-1 expression is correlated with the histological grade of malignancy at the deep invasive front in oral squamous cell carcinoma, J. Oral Pathol. Med. 35 (2006) 301–306.

[16] T. Kuzume, I. Kubonishi, S. Takeuchi, T. Takeuchi, J. Iwata, H. Sonobe, Y. Ohtsuki, I. Miyoshi, Establishment and characterization of a thymic carcinoma cell line (Ty-82) carrying t(15;19)(q15;p13) chromosome abnormality, Int. J. Cancer 50 (1992) 259–264.

[17] A. Martinez, M.L. Spencer, U. Brethauer, P. Grez, F.J. Marchesani, I.G. Rojas, Reduction of syndecan-1 expression during lip carcinogenesis, J. Oral Pathol. Med. 38 (2009) 580–583.

[18] T. Soukka, J. Pohjola, P. Inki, R.P. Happonen, Reduction of syndecan-1 expression is associated with dysplastic oral epithelium, J. Oral Pathol. Med. 29 (2000) 308–313.

[19] E.B. Stelow, A.M. Bellizzi, K. Taneja, S.E. Mills, R.D. Legallo, J.L. Kutok, J.C. Aster, C.A. French, NUT rearrangement in undifferentiated carcinomas of the upper aerodigestive tract, Am. J. Surg. Pathol. 32 (2008) 828–834.

[20] E.B. Stelow, A review of NUT midline carcinoma, Head Neck Pathol. 5 (2011) 31–35.

[21] H. Sugimura, Detection of chromosome changes in pathology archives: an application of microwave-assisted fluorescence in situ hybridization to human carcinogenesis studies, Carcinogenesis 29 (2008) 681–687.
[22] H. Sugimura, H. Mori, K. Nagura, S. Kiyose, H. Tao, M. Isozaki, H. Igarashi, K. Shinmura, A. Hasegawa, Y. Kitayama, F. Tanioka, Fluorescence in situ hybridization analysis with a tissue microarray: 'FISH and chips' analysis of pathology archives, Pathol. Int. 60 (2010) 543–550.
[23] M. Tanaka, K. Kato, K. Gomi, M. Yoshida, T. Niwa, N. Aida, H. Kigasawa, Y. Ohama, Y. Tanaka, NUT midline carcinoma: report of 2 cases suggestive of pulmonary origin, Am. J. Surg. Pathol. 36 (2012) 381–388.

Hindawi Publishing Corporation
Oxidative Medicine and Cellular Longevity
Volume 2014, Article ID 617351, 12 pages
http://dx.doi.org/10.1155/2014/617351

Research Article

Impaired 8-Hydroxyguanine Repair Activity of MUTYH Variant p.Arg109Trp Found in a Japanese Patient with Early-Onset Colorectal Cancer

Kazuya Shinmura,[1] Masanori Goto,[1,2] Hong Tao,[1] Hisami Kato,[1] Rie Suzuki,[1] Satoki Nakamura,[1] Tomonari Matsuda,[3] Guang Yin,[4] Makiko Morita,[4] Suminori Kono,[4] and Haruhiko Sugimura[1]

[1] *Department of Tumor Pathology, Hamamatsu University School of Medicine, 1-20-1 Handayama, Higashi Ward, Hamamatsu, Shizuoka 431-3192, Japan*
[2] *Division of Cancer Development System, National Cancer Center Research Institute, Tokyo 104-0045, Japan*
[3] *Research Center for Environmental Quality Management, Kyoto University, Shiga 520-0811, Japan*
[4] *Department of Preventive Medicine, Graduate School of Medical Sciences, Kyushu University, Fukuoka 812-8582, Japan*

Correspondence should be addressed to Kazuya Shinmura; kzshinmu@hama-med.ac.jp

Received 29 November 2013; Revised 5 February 2014; Accepted 11 February 2014; Published 23 March 2014

Academic Editor: Antonio Ayala

Purpose. The biallelic inactivation of the 8-hydroxyguanine repair gene *MUTYH* leads to MUTYH-associated polyposis (MAP), which is characterized by colorectal multiple polyps and carcinoma(s). However, only limited information regarding MAP in the Japanese population is presently available. Since early-onset colorectal cancer (CRC) is a characteristic of MAP and might be caused by the inactivation of another 8-hydroxyguanine repair gene, *OGG1*, we investigated whether germline *MUTYH* and *OGG1* mutations are involved in early-onset CRC in Japanese patients. *Methods.* Thirty-four Japanese patients with early-onset CRC were examined for germline *MUTYH* and *OGG1* mutations using sequencing. *Results.* Biallelic pathogenic mutations were not found in any of the patients; however, a heterozygous p.Arg19* *MUTYH* variant and a heterozygous p.Arg109Trp *MUTYH* variant were detected in one patient each. The p.Arg19* and p.Arg109Trp corresponded to p.Arg5* and p.Arg81Trp, respectively, in the type 2 nuclear-form protein. The defective DNA repair activity of p.Arg5* is apparent, while that of p.Arg81Trp has been demonstrated using DNA cleavage and *supF* forward mutation assays. *Conclusion.* These results suggest that biallelic *MUTYH* or *OGG1* pathogenic mutations are rare in Japanese patients with early-onset CRC; however, the p.Arg19* and p.Arg109Trp *MUTYH* variants are associated with functional impairments.

1. Introduction

8-Hydroxyguanine (8OHG) is an oxidized form of guanine, and the formation of 8OHG in DNA causes a G:C to T:A mutation, since 8OHG can pair with adenine as well as cytosine [1, 2]. To prevent such mutations in human cells, MUTYH (MIM #604933) and OGG1 (MIM #601982) proteins are involved in DNA glycosylase-initiating base excision repair, which is a component of the human DNA repair system [3–8]. MUTYH catalyzes the removal of adenine mispaired with 8OHG in double-stranded DNA, and OGG1 catalyzes the removal of 8OHG at the 8OHG:C site. Regarding MUTYH, multiple forms, including two major forms (type 1 mitochondrial form and type 2 nuclear form), are expressed in human cells [3–6].

Clinically, biallelic germline inactivating *MUTYH* mutations are known to predispose an individual to MUTYH-associated polyposis (MAP: MIM #608456), a hereditary disorder characterized by multiple colorectal polyps and carcinoma(s) [9–11]. Various pathogenic *MUTYH* mutations, including two major mutations (p.Tyr179Cys and p.Gly396Asp), have been detected in MAP patients in several

ethnic populations [12]; however, neither the p.Tyr179Cys nor the p.Gly396Asp mutation has been found in the Japanese population [13–15], and which *MUTYH* variations are the major pathogenic mutations in the Japanese population remains unclear. In accordance with the notion that early-onset cancer is likely to be associated with the germline abnormality of certain gene(s) [16], early-onset colorectal cancer (CRC) is one of the characteristics of MAP [12], and early-onset CRC is thought to occur in patients with biallelic-inactivating mutations of another 8OHG repair gene, *OGG1*. Therefore, we hypothesized that biallelic inactivating mutations of *MUTYH* or *OGG1* might lead to early-onset CRC in Japanese patients. To test this hypothesis, we examined 34 Japanese patients with early-onset CRC for germline *MUTYH* and *OGG1* mutations. Then, we investigated whether the detected variants were associated with defective 8OHG repair activity.

2. Materials and Methods

2.1. Clinical Samples and Cell Line. Blood specimens from 685 CRC cases and 778 controls were collected in a previous study [17]. Written informed consent was obtained from each individual patient [17]. The characteristics of the cases and the controls have been described previously [17, 18]. Briefly, the cases were composed of a consecutive series of patients with histologically confirmed incident colorectal adenocarcinomas, and the controls were composed of individuals that had no diagnosis of CRC. Additionally, the cases had no prior history of removal of the colorectum, familial adenomatous polyposis (FAP: MIM #175100), or inflammatory bowel disease (IBD). All the cases and the controls had been previously genotyped for c.36+11C>T, c.504+35A>G, c.934−2A>G, and c.1014G>C *MUTYH* polymorphisms [19], but none had been sequenced for the whole coding exons of the *MUTYH* and *OGG1* genes. A human cancer cell line, H1299, was obtained from the American Type Culture Collection (Manassas, VA). The H1299 cells and their derivatives were maintained at 37°C in RPMI1640 medium supplemented with 10% fetal bovine serum (Equitech-Bio, Kerrville, TX) and penicillin/streptomycin under a 5% CO_2 atmosphere. The study design was approved by the institutional review boards.

2.2. PCR-Sequencing Analysis. Genomic DNA was extracted as described previously [17]. All the coding exons of the *MUTYH* and *OGG1* genes and their boundary regions were amplified using PCR with HotStarTaq DNA polymerase (Qiagen, Valencia, CA). The PCR primer sequences of *MUTYH* and *OGG1* are summarized in Supplementary Tables S1 and S2 in the Supplementary Material available online at http://dx.doi.org/10.1155/2014/617351, respectively. The PCR-amplified products were directly sequenced with a BigDye Terminator Cycle Sequencing Reaction Kit (Applied Biosystems, Tokyo, Japan) and an ABI 3130 Genetic Analyzer (Applied Biosystems).

2.3. PCR with Confronting Two-Pair Primers (PCR-CTPP) Analysis. Genotyping of the c.55C>T and c.325C>T variants was performed using a PCR-CTPP analysis, as described previously [20]. The PCR primer sequences are summarized in Supplementary Table S3. The PCR products were fractionated by electrophoresis on a 2.0% agarose gel and were stained with ethidium bromide.

2.4. Construction of Expression Plasmid. Plasmid vectors for the expression of human wild-type (WT) MUTYH type 2 in *Escherichia coli* (*E. coli*) and human cells were previously constructed by inserting the cDNA into a pET25b(+) vector (Novagen, Darmstadt, Germany) and a piggyBac cumate switch inducible vector (System Biosciences, Mountain View, CA), respectively [21, 22]. Expression vectors for the MUTYH variants were generated using site-directed mutagenesis with a QuikChange Site-directed Mutagenesis kit (Stratagene, La Jolla, CA).

2.5. Preparation of Recombinant Protein. *E. coli* BL21-CodonPlus (DE3)-RP competent cells (Stratagene) were transformed with the MUTYH-pET25b vector and cultured at 37°C until an A_{600} of 0.6. After incubation with 0.1 mM IPTG at 15°C for 12 h, MUTYH-His_6 protein was purified with TALON metal affinity resins (Clontech, Palo Alto, CA) and a TALON 2 mL disposable gravity column (Clontech). The protein was then dialyzed against buffer containing 10 mM sodium phosphate (pH 7.6), 50 mM NaCl, 0.5 mM DTT, 0.1 mM EDTA, 0.5 mM PMSF, 2 μg/mL pepstatin, 2 μg/mL leupeptin, 50 μM chymostatin, and 10% glycerol. The quality and concentration of MUTYH proteins were determined by resolving the proteins with SDS-polyacrylamide gel electrophoresis (PAGE) and staining them with Coomassie Brilliant Blue (CBB); Image J software (National Institutes of Health, Bethesda, MD) was then used for quantification.

2.6. Western Blot Analysis. A Western blot analysis using a mouse anti-MUTYH monoclonal antibody (4D10; Abnova, Taipei, Taiwan) or an anti-β-tubulin monoclonal antibody (clone 2-28-33; Sigma-Aldrich, St. Louis, MO) was performed as described previously [22, 23].

2.7. DNA Cleavage Assay. First, 30-mer oligonucleotides containing or not containing a single 8OHG (5′-CTG GTG GCC TGA C[8OHG or T]C ATT CCC CAA CTA GTG-3′) were chemically synthesized and purified using PAGE (Japan Bio Services, Saitama, Japan). Complementary oligonucleotides containing an adenine opposite the 8OHG or T were ^{32}P-labeled at the 5′ terminus with a MEGALABEL kit (Takara, Osaka, Japan) and [γ-^{32}P]ATP (PerkinElmer, Tokyo, Japan), and these oligonucleotides were then annealed to oligonucleotides containing a single 8OHG or T. A reaction mixture containing 20 mM sodium phosphate (pH 7.6), 100 mM NaCl, 0.5 mM DTT, 0.5 mM EDTA, 5 μM $ZnCl_2$, 1.5% glycerol, 2.5 nM labeled oligonucleotide, 50 μg/mL BSA, and 90 fmoles of MUTYH protein was then incubated at 37°C for 15 min, and the mixture was treated with 0.1 M NaOH. After the mixture was denatured, it was subjected to 20% PAGE. A

^{32}P-labeled marker oligonucleotide was used as a size marker for the cleavage products. The radioactivities of the intact and cleaved oligonucleotides were quantified using an FLA-3000 fluoroimage analyzer (Fuji Film, Tokyo, Japan) and ImageGauge software (Fuji Film).

2.8. Establishment of Stable Inducible Cell Lines. H1299 cells were transfected with the piggyBac cumate switch inducible vector for MUTYH expression together with the piggyBac transposase vector (System Biosciences). To establish stable inducible cell lines, positively transposed cells were selected using puromycin (1 μg/mL). Since the inducible piggyBac vector features a tight cumate switch combined with an EF1-CymR repressor-T2A-Puro cassette to establish stable cell lines, the addition of cumate solution (System Biosciences) to the puromycin-selected cells leads to the induction of MUTYH expression.

2.9. Indirect Immunofluorescence Analysis. Cells were fixed with 10% formalin at room temperature, permeabilized with 1% Nonidet P-40, blocked with 10% normal goat serum, and probed with mouse anti-MUTYH monoclonal antibody (4D10; Abnova). Indirect immunofluorescence labeling was performed by exposure to an Alexa Fluor 594-conjugated secondary antibody (Molecular Probes, Eugene, OR), and the nuclei were stained with 4′,6-diamidino-2-phenylindole (DAPI) (Sigma-Aldrich). The slides were promptly examined under a fluorescence microscope (Olympus BX-51-FL; Olympus, Tokyo, Japan) equipped with epifluorescence filters and a photometric CCD camera (Sensicam; PCO Company, Kelheim, Germany). The images captured were digitized and stored in the image analysis program (MetaMorph; Molecular Devices, Palo Alto, CA).

2.10. supF Forward Mutation Assay. A single 8OHG:C mispair was introduced at nucleotide position 159 of the bacterial suppressor tRNA (*supF*) gene of the shuttle vector plasmid pMY189, as described previously [22–24]. A *supF* forward mutation assay for H1299-derived cells was performed using the 8OHG-containing pMY189 plasmid and the KS40/pKY241 indicator *E. coli* strain, as described previously [22, 23]. The mutation frequencies were calculated as the number of *E. coli supF* mutants per total number of *E. coli* transformants. The mutations in the *supF* gene were then analyzed as described previously [22].

2.11. Computational Analysis for Variants. The functional effects of nonsynonymous variants were predicted by the online software tools PolyPhen-2 [25], SIFT [26], and PROVEAN [27]. The allele frequencies of variants in a large number of Japanese individuals were examined using a reference database of genetic variations in the Japanese population (http://www.genome.med.kyoto-u.ac.jp/SnpDB/).

2.12. Statistical Analysis. The statistical analyses were performed using an unpaired *t*-test, Dunnett test, or Fisher exact test. JMP version 9 software (SAS Institute, Cary, NC) was used for all the statistical analyses. *P* values less than 0.05 were considered statistically significant.

3. Results

3.1. Identification of p.Arg19 and p.Arg109Trp MUTYH Variants in Japanese Patients with Early-Onset CRC.* To investigate whether germline mutations of the DNA glycosylase genes *MUTYH* and *OGG1* are involved in early-onset CRC in Japanese patients, we attempted to utilize a population of 685 Japanese CRC patients. Among them, we selected 34 CRC patients with the lowest ages of onset (corresponding to 5% of the total patient population) (Table 1). All 34 CRC patients were less than 43 years old and had no history of FAP or IBD. We then examined the 34 CRC patients for germline *MUTYH* and *OGG1* mutations by sequencing every coding exon of both genes. As a result, 9 *MUTYH* variants and 7 *OGG1* variants were found (Table 2, Figure 1(a)), and the genotype and allele frequencies of the nucleotide variations are summarized in Table 2 and the characteristics of the variations are summarized in Table 3. Genotypes of the variations in the coding region and splice-site region in 34 patients are also summarized in Supplementary Tables S4 and S5. Among the 9 *MUTYH* variants, although c.36+11C>T, c.504+35A>G, c.934−2A>G, c.1014G>C (p.Gln338His), c.1118C>T (p.Ala373Val), c.1431G>C (p.Thr477Thr), and c.1477−40C>G are not considered to be MAP pathogenic alleles, the remaining two variants of c.55C >T (p.Arg19*) and c.325C>T (p.Arg109Trp) were identical to variants previously found in one patient each with colorectal multiple adenomas and a carcinoma [28]. In our study, the p.Arg19* variant was detected in one patient as a heterozygous status for the wild-type and variant alleles, and the p.Arg109Trp variant was also detected heterozygously in one patient. Moreover, the p.Arg19* variant encodes a truncating protein, and the p.Arg109Trp variant encodes a protein with the substitution of a highly conserved amino acid, p.Arg109 (National Center for Biotechnology Information, Bethesda, MD) (Figure 1(b)); the missense protein was predicted to be functionally damaged by the PolyPhen-2, SIFT, and PROVEAN software programs (Table 3). Therefore, we considered the two variants to be candidate MAP pathogenic alleles. Regarding the 7 *OGG1* variants, c.949−89G>T and c.966C>T (p.Asp322Asp) were novel (Supplementary Figure S1); however, since the former exists in an intron and the latter is a synonymous variation, these variants were not considered to be pathogenic mutations. Among the other 5 *OGG1* variants, c.−18G>T and c.977C>G (p.Ser326Cys) have been reported as low-penetrance cancer susceptibility variants [29, 30], while the remaining three were untranslated, synonymous, or intronic variations, meaning that all of them are not highly pathogenic mutations. Therefore, none of the patients were thought to have biallelic pathogenic *MUTYH* or *OGG1* mutations in the presently studied early-onset CRC group. However, we decided to further investigate the p.Arg19* and p.Arg109Trp *MUTYH* variants as candidate pathogenic alleles.

Table 1: Clinicopathological profiles of 34 Japanese patients with early-onset CRC.

Case number	Age	Sex	Tumor site	Tumor histology	Tumor stage
1	27	F	Distal colon	Mucinous adenocarcinoma	II
2	29	F	Proximal colon	WD adenocarcinoma[a]	II
3	34	F	Distal colon	WD adenocarcinoma	I
4	36	M	Distal colon	WD adenocarcinoma	IIIa
5	39	F	Rectum	MD adenocarcinoma[b]	IIIa
6	39	F	Distal colon	WD adenocarcinoma	IV
7	38	M	Proximal colon	MD adenocarcinoma	II
8	36	F	Distal colon	MD adenocarcinoma	IIIb
9	39	F	Rectum	WD adenocarcinoma	IIIa
10	39	M	Proximal colon	WD adenocarcinoma	IIIb
11	37	F	Proximal colon	WD adenocarcinoma	I
12	33	F	Proximal colon	WD adenocarcinoma	IIIa
13	36	M	Rectum	WD adenocarcinoma	I
14	35	M	Distal colon	MD adenocarcinoma	II
15	37	M	Proximal colon	MD adenocarcinoma	IIIb
16	38	M	Rectum	WD adenocarcinoma	II
17	43	M	Rectum	WD adenocarcinoma	I
18	41	F	Distal colon	WD adenocarcinoma	II
19	41	M	Distal colon	MD adenocarcinoma	IIIb
20	42	M	Rectum	WD adenocarcinoma	IIIb
21	40	M	Proximal colon	WD adenocarcinoma	I
22	43	F	Proximal colon	MD adenocarcinoma	II
23	42	M	Rectum	MD adenocarcinoma	IIIa
24	42	M	Proximal colon	MD adenocarcinoma	I
25	42	M	Rectum	WD adenocarcinoma	I
26	43	M	Rectum	PD adenocarcinoma[c]	IV
27	43	M	Distal colon	WD adenocarcinoma	IIIa
28	41	M	Rectum	MD adenocarcinoma	II
29	42	M	Rectum	WD adenocarcinoma	IIIa
30	40	M	Rectum	MD adenocarcinoma	II
31	43	M	Distal colon	WD adenocarcinoma	I
32	43	M	Distal colon	WD adenocarcinoma	II
33	42	M	Proximal colon	WD adenocarcinoma	II
34	40	M	Rectum	MD adenocarcinoma	IIIb

[a]Well-differentiated adenocarcinoma. [b]Moderately differentiated adenocarcinoma. [c]Poorly differentiated adenocarcinoma.

3.2. Absence of p.Arg19 and p.Arg109Trp MUTYH Variants in Japanese Individuals without CRC.* To determine the frequency of the p.Arg19* and p.Arg109Trp *MUTYH* variants in Japanese individuals without CRC, we genotyped both nucleotide variations using PCR-CTPP in as many as 100 individuals randomly selected from the control group (Figures 1(c) and 1(d)). Since the above-described cases with a p.Arg19* or p.Arg109Trp variant exhibited a heterozygous pattern of the WT and variant alleles, these cases were used as positive controls in the PCR-CTPP analysis. The results showed that none of the controls exhibited p.Arg19* or p.Arg109Trp variants, suggesting that p.Arg19* and p.Arg109Trp are rare variants in the Japanese population.

3.3. Defective DNA Glycosylase Activity of MUTYH Type 2 p.Arg81Trp Variant. To conclude whether a *MUTYH* variant allele is pathogenic, an impairment in the repair activity of the protein based on the nucleotide variant must be evident. p.Arg19* and p.Arg109Trp correspond to p.Arg5* and p.Arg81Trp, respectively, in the type 2 nuclear-form protein, which is the major MUTYH form in human cells. Since p.Arg5* has a length of only 5 amino acids, compared with 521 amino acids in the full-length type 2 protein, the DNA repair activity of p.Arg5* is most likely defective. On the other hand, p.Arg81Trp yields a missense form, and the repair activity of the mutant protein has not yet been analyzed. Thus, we planned to evaluate the DNA glycosylase activity of the p.Arg81Trp protein by comparing the cleavage activity of the mutant with that of the WT protein in the presence of an A:8OHG mismatch-containing DNA substrate. We also planned to utilize the p.Asp208Asn mutant as a negative control in the comparison [21]. First, the WT, p.Arg81Trp,

Table 2: Genotype and allele frequencies of the *MUTYH* and *OGG1* nucleotide variations found in 34 Japanese patients with early-onset colorectal carcinoma.

Gene	Variant	Nucleotide		Genotype frequency			Allele frequency	
		wt	vt	wt/wt	wt/vt	vt/vt	wt	vt
MUTYH	c.36+11C>T	C	T	32 (94.1%)	2 (5.9%)	0 (0%)	66 (97.1%)	2 (2.9%)
MUTYH	c.55C>T (p.Arg19*)	C	T	33 (97.1%)	1 (2.9%)	0 (0%)	67 (98.5%)	1 (1.5%)
MUTYH	c.325C>T (p.Arg109Trp)	C	T	33 (97.1%)	1 (2.9%)	0 (0%)	67 (98.5%)	1 (1.5%)
MUTYH	c.504+35A>G	A	G	25 (73.5%)	9 (26.5%)	0 (0%)	59 (86.8%)	9 (13.2%)
MUTYH	c.934−2A>G	A	G	33 (97.1%)	1 (2.9%)	0 (0%)	67 (98.5%)	1 (1.5%)
MUTYH	c.1014G>C (p.Gln338His)	G	C	15 (44.1%)	15 (44.1%)	4 (11.8%)	45 (66.2%)	23 (33.8%)
MUTYH	c.1118C>T (p.Ala373Val)	C	T	33 (97.1%)	1 (2.9%)	0 (0%)	67 (98.5%)	1 (1.5%)
MUTYH	c.1431G>C (p.Thr477Thr)	G	C	32 (94.1%)	2 (5.9%)	0 (0%)	66 (97.1%)	2 (2.9%)
MUTYH	c.1477−40C>G	C	G	2 (5.9%)	7 (20.6%)	25 (73.5%)	11 (16.2%)	57 (83.8%)
OGG1	c.−23A>G	A	G	32 (94.1%)	2 (5.9%)	0 (0%)	66 (97.1%)	2 (2.9%)
OGG1	c.−18G>T	G	T	32 (94.1%)	2 (5.9%)	0 (0%)	66 (97.1%)	2 (2.9%)
OGG1	c.294G>A (p.Lys98Lys)	G	A	33 (97.1%)	1 (2.9%)	0 (0%)	67 (98.5%)	1 (1.5%)
OGG1	c.748−15C>G	C	G	13 (38.2%)	14 (41.2%)	7 (20.6%)	40 (58.8%)	28 (41.2%)
OGG1	c.949−89G>T	G	T	33 (97.1%)	1 (2.9%)	0 (0%)	67 (98.5%)	1 (1.5%)
OGG1	c.966C>T (p.Asp322Asp)	C	T	33 (97.1%)	1 (2.9%)	0 (0%)	67 (98.5%)	1 (1.5%)
OGG1	c.977C>G (p.Ser326Cys)	C	G	11 (32.4%)	17 (50.0%)	6 (17.6%)	39 (57.4%)	29 (42.6%)

wt: wild-type, vt: variant type.

and p.Asp208Asn recombinant proteins were expressed in *E. coli* and were purified to a high level of homogeneity (Figure 2(a)). Their molecular size of approximately 61 kDa was determined using SDS-PAGE/CBB staining and Western blot analysis, and this size corresponded to the size calculated from the cDNA sequence (Figures 2(a) and 2(b)). Then, the DNA glycosylase activity of the MUTYH proteins was examined by determining its capacity to cleave a double-stranded oligonucleotide containing an adenine mispaired with 8OHG (Figure 2(c)). No clear cleavage products were detected when an oligonucleotide containing an unmodified A:T base pair was exposed to any of the MUTYH proteins, but cleavage products with the same mobility as the marker oligonucleotide were detected when WT MUTYH protein, but not a p.Asp208Asn negative control protein, was allowed to react with an oligonucleotide containing an A:8OHG base pair (Figures 2(d) and 2(e)). Importantly, a significantly smaller amount of cleavage products was detected in the reaction with p.Arg81Trp than in the reaction with WT (% incision: 1.8% versus 29.3%) (Figures 2(d) and 2(e)). These results indicate that the DNA glycosylase activity of p.Arg81Trp was severely decreased.

3.4. Impaired Suppressive Activity of MUTYH Type 2 p.Arg81Trp Variant against Mutations Caused by 8OHG. To investigate the ability of MUTYH p.Arg81Trp variant to suppress mutations caused by 8OHG in human cells, we planned to use the piggyBac transposon vector system [31] to establish human cells capable of inducibly expressing MUTYH protein and to perform a *supF* forward mutation assay using the shuttle plasmid pMY189, which contains a single 8OHG in the *supF* gene. First, we established human H1299 cell lines capable of inducibly expressing WT, p.Arg81Trp, or p.Asp208Asn MUTYH using the piggyBac transposon vector system [31]. The expression of MUTYH protein after cumate induction was examined using a Western blot analysis with an anti-MUTYH monoclonal antibody (Figure 3(a)). MUTYH protein was abundantly expressed in cells in which a WT, p.Arg81Trp, or p.Asp208Asn MUTYH expression vector, but not an empty vector, was transposed. An immunofluorescence analysis also showed abundant MUTYH protein expression in cells in which a WT, p.Arg81Trp, or p.Asp208Asn MUTYH expression vector, but not an empty vector, was transposed (Figure 3(b)). The p.Arg81Trp variant, as well as the WT MUTYH protein, was localized in the nucleus, suggesting that the amino acid changes in p.Arg81Trp were unlikely to alter the subcellular localization of the protein in human cells.

Next, the mutation frequencies were compared among the empty vector-transposed human cells and the cumate-inducible stable cells expressing WT or a variant MUTYH

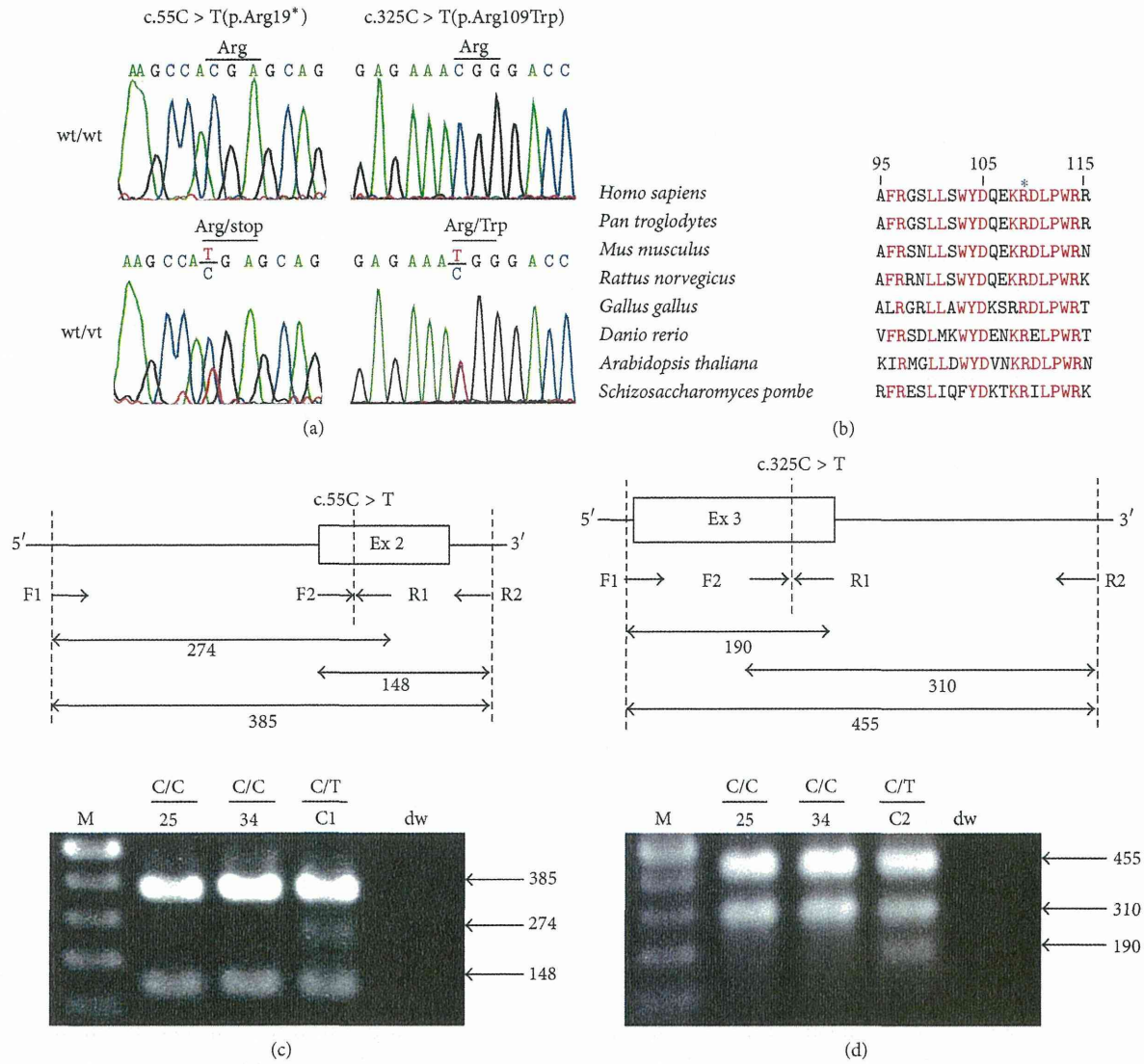

FIGURE 1: Identification and genotyping of c.55C>T (p.Arg19*) and c.325C>T (p.Arg109Trp) variants of the *MUTYH* gene in the Japanese population. (a) Identification of c.55C>T and c.325C>T variants of the *MUTYH* gene in Japanese patients with early-onset CRC. Sequencing electropherograms show a C to T variation at the c.55 and c.325 positions (lower panels). (b) Amino acid sequence alignment of a section of MUTYH among different species. The human MUTYH protein sequence from p.Ala95 to p.Arg115 was compared with the MUTYH sequences of other species. Amino acids exhibiting ≥75% identity among the species are shown in red. The position of p.Arg109 is marked by an asterisk. (c and d) Genotyping of the c.55C>T (c) and c.325C>T (d) variants of the *MUTYH* gene in Japanese individuals without CRC (control individuals). The schematic diagrams of PCR-CTPP used to genotype the c.55C>T and c.325C>T variants are shown in the upper panel. The PCR primers are indicated by the horizontal arrows; and F and R mean forward primer and reverse primer, respectively. The location of each variant is indicated by a vertical dashed line. The PCR product sizes for the primer pairs of F1 and R1, F2 and R2, and F1 and R2 are shown. Representative results of agarose gel electrophoresis of the PCR-CTPP products are shown in the lower panel. The number on the panel indicates the assigned number of control individuals, "C1" and "C2" indicate a case with a variant allele, and "dw" indicates the no template DNA in the PCR. M indicates a size marker.

using a *supF* forward mutation assay with the shuttle plasmid pMY189. In this assay, we introduced a single 8OHG residue at position 159 of the *supF* gene in pMY189. The mutation frequency of *supF* was 3.2×10^{-2} in the 8OHG-containing pMY189 plasmid and 2.3×10^{-4} in the WT pMY189 in empty vector-transposed cells (Figure 3(c)), representing a 139-fold increase in the mutation frequency with the introduction of 8OHG. The mutation frequency of *supF* in the 8OHG-containing pMY189 plasmid in the WT MUTYH-transposed and p.Arg81Trp variant-transposed, but not p.Asp208Asn-transposed, cells was significantly lower than that in the empty vector-transposed cells (Figure 3(c)). Importantly, the